





# High-speed plasmonic modulator in a single metal layer

## Journal Article

### Author(s):

Ayata, Masafumi; Fedoryshyn, Yuriy M.; Heni, Wolfgang; [Bäuerle, Benedikt](#) ; [Josten, Arne](#) ; Zahner, Marco; [Koch, Ueli](#) ; Salamin, Yannick; Hössbacher, Claudia; Haffner, Christian; Elder, Delwin L.; Dalton, Larry R.; [Leuthold, Juerg](#) 

### Publication date:

2017-11-03

### Permanent link:

<https://doi.org/10.3929/ethz-b-000222814>

### Rights / license:

[In Copyright - Non-Commercial Use Permitted](#)

### Originally published in:

Science 358(6363), <https://doi.org/10.1126/science.aan5953>

### Funding acknowledgement:

688166 - A generic CMOS-compatible platform for co-integrated plasmonics/photronics/electronics PICs towards volume manufacturing of low energy, small size and high performance photonic devices (SBFI)

670478 - Plasmonic-Silicon-Organic Hybrid – a Universal Platform for THz Communications (EC)

# High-speed plasmonic modulator in a single metal layer

Ayata, Masafumi; Fedoryshyn, Yuriy M.; Heni, Wolfgang; Bäuerle, Benedikt; Josten, Arne; Zahner, Marco; Koch, Ueli; Salamin, Yannick; Hössbacher, Claudia; Haffner, Christian; Elder, Delwin L.; Dalton, Larry R.; Leuthold, Juerg

## Ultrafast plasmonic modulation

Plasmonics converts light into propagating electrical signals. This approach could allow us to shrink optical components to the nanometer scale, far below the hundreds of wavelengths typically set by conventional optics. Ayata *et al.* fabricated a plasmonic modulator from a single layer of gold using a substrate-independent process. They created a device with a footprint less than the cross-sectional area of a human hair and with modulation rates exceeding 100 GHz, which could provide a flexible platform for future ultrafast plasmonic technology.

## Abstract

Plasmonics provides a possible route to overcome both the speed limitations of electronics and the critical dimensions of photonics. We present an all-plasmonic 116-gigabits per second electro-optical modulator in which all the elements—the vertical grating couplers, splitters, polarization rotators, and active section with phase shifters—are included in a single metal layer. The device can be realized on any smooth substrate surface and operates with low energy consumption. Our results show that plasmonics is indeed a viable path to an ultracompact, highest-speed, and low-cost technology that might find many applications in a wide range of fields of sensing and communications because it is compatible with and can be placed on a wide variety of materials.

Applied plasmonics has been proposed as an alternative to conventional photonics and electronics to overcome their bottlenecks in terms of speed and energy efficiency, as well as manufacturing cost and footprint ([1–3](#)). A large variety of plasmonic structures and devices—including passive waveguides and active components such as light emitters, detectors, and modulators—have been investigated and demonstrated ([4–22](#)). Plasmonic devices are continuously gaining interest for applications ranging from sensing to telecommunications ([23–28](#)).

Among the many plasmonic devices, the optical modulator plays a central role by mapping a received electrical signal onto an optical carrier ([29](#)). Various types of plasmonic modulators have been introduced that exploit the free-carrier dispersion effect ([11–15](#)), thermo-optic effect ([16](#), [17](#)), mechanical effect ([18](#), [19](#)), or Pockels effect ([20–22](#)) with the strong confinement of light in the active region so that they can be operated on a small device footprint. In telecommunications, the Pockels-effect Mach-Zehnder modulators have been preferred because they allow one to encode electrical information either onto the phase or the amplitude of an optical carrier, thus making it a key building block of any state-of-the-art modulator for advanced modulation formats ([30](#)). To date, Pockels-effect plasmonic devices have demonstrated operation beyond 100 Gbit/s with power consumption of 25 fJ/bit ([21](#), [31](#)). However, these devices rely partially on photonic waveguides to bring light onto the chip, which results in a large footprint and requires dedicated substrates. An all-metallic Mach-Zehnder modulator that could be placed on almost any surface and that could couple the optical signal directly to a fiber would mark quite an advance.

We present an integrated plasmonic Mach-Zehnder modulator that only relies on metallic structures fabricated on a glass layer and performs high-speed modulation. The entire device is produced in a single metal layer covered with a nonlinear optical material, and it occupies an area of 36  $\mu\text{m}$  by 6  $\mu\text{m}$ . High-speed modulation enables data transmission beyond 116 Gbit/s at a bit-error ratio (BER) of less than  $1.7 \times 10^{-3}$ . The input and output optical signals are fed in and fed out through a single multicore fiber (MCF) via a new coupler that performs vertical grating coupling, polarization rotation, and splitting in one

compact metallic structure so that devices can be arranged with a pitch only limited by the distance of the next fiber core.

The all-metallic high-speed plasmonic modulator is arranged in a Mach-Zehnder interferometer (MZI) configuration with vertical metallic grating couplers and polarization rotators (Fig. 1). Modulation occurs in the slots of the two MZI arms, which are filled with a nonlinear optical (NLO) material. When electrical signals are fed to the central part of the device (the grating coupler serves as a signal pad that becomes the inner plasmonic rail, whereas the outer plasmonic rails also serve as ground pads), electric fields are applied across the two slots in opposite directions. Due to the Pockels effect, the light propagates faster in one of the MZI arms and slower in the other, depending on the directions of the applied electric fields. At the output of the MZI, both portions of the optical carrier from the two arms are rotated back to p-polarization while having constructive or destructive interference based on the sign of the applied electrical signals. The optical signal, now encoded with information, is then coupled out to another core of the MCF via the output vertical metallic grating coupler. The entire device, comprising the vertical grating couplers, the polarization rotators, and the plasmonic Mach-Zehnder phase shifters, can be realized in a single metal layer (Fig. 2A), and it occupies an area defined by the distance between two cores of a MCF.

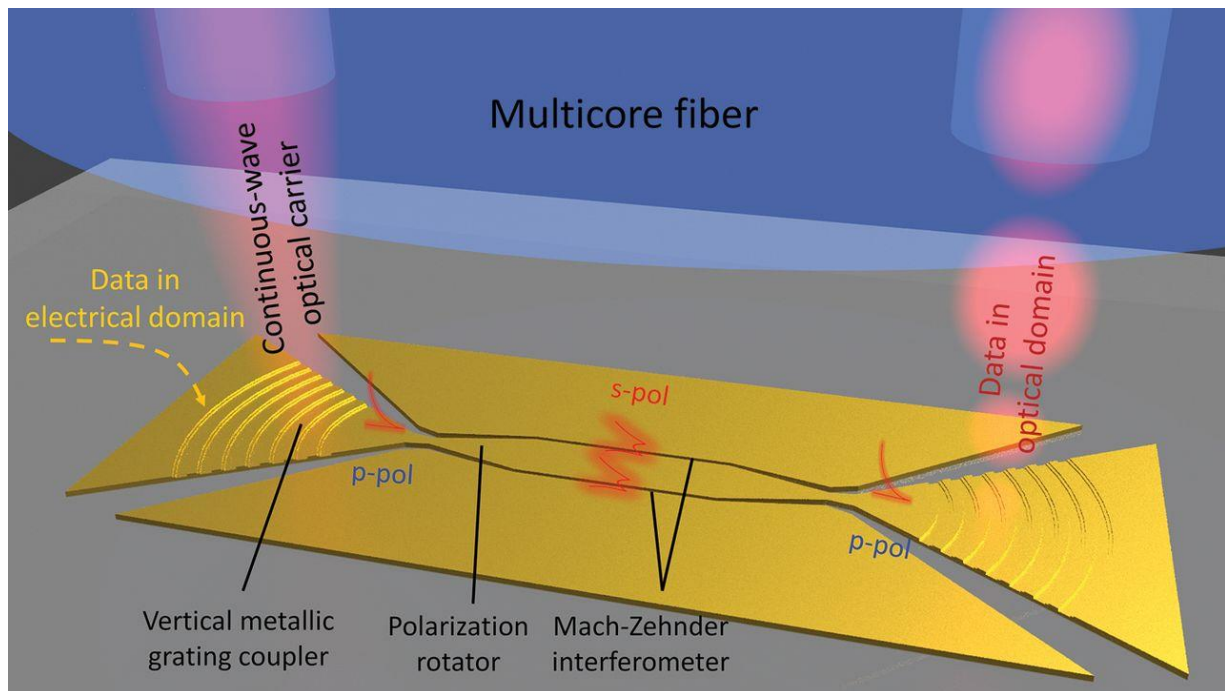


Fig. 1 All-metallic high-speed modulator.

Schematic of the operation principle of an all-metallic modulator in a MZI configuration with vertical metallic grating couplers and polarization rotators. A continuous-wave optical carrier is coupled into the device through the vertical metallic grating coupler from one core of the multicore fiber. The polarization of the optical carrier is rotated from p-polarization (p-pol) to s-polarization (s-pol) and split into the arms of the MZI in the polarization rotator section. The electrical information is then encoded by means of a phase shift through the Pockels effect onto the two optical signals in the MZI arms. At the output, the two optical signals from the arms interfere either constructively or destructively, and they are coupled back to another core of the multicore fiber.

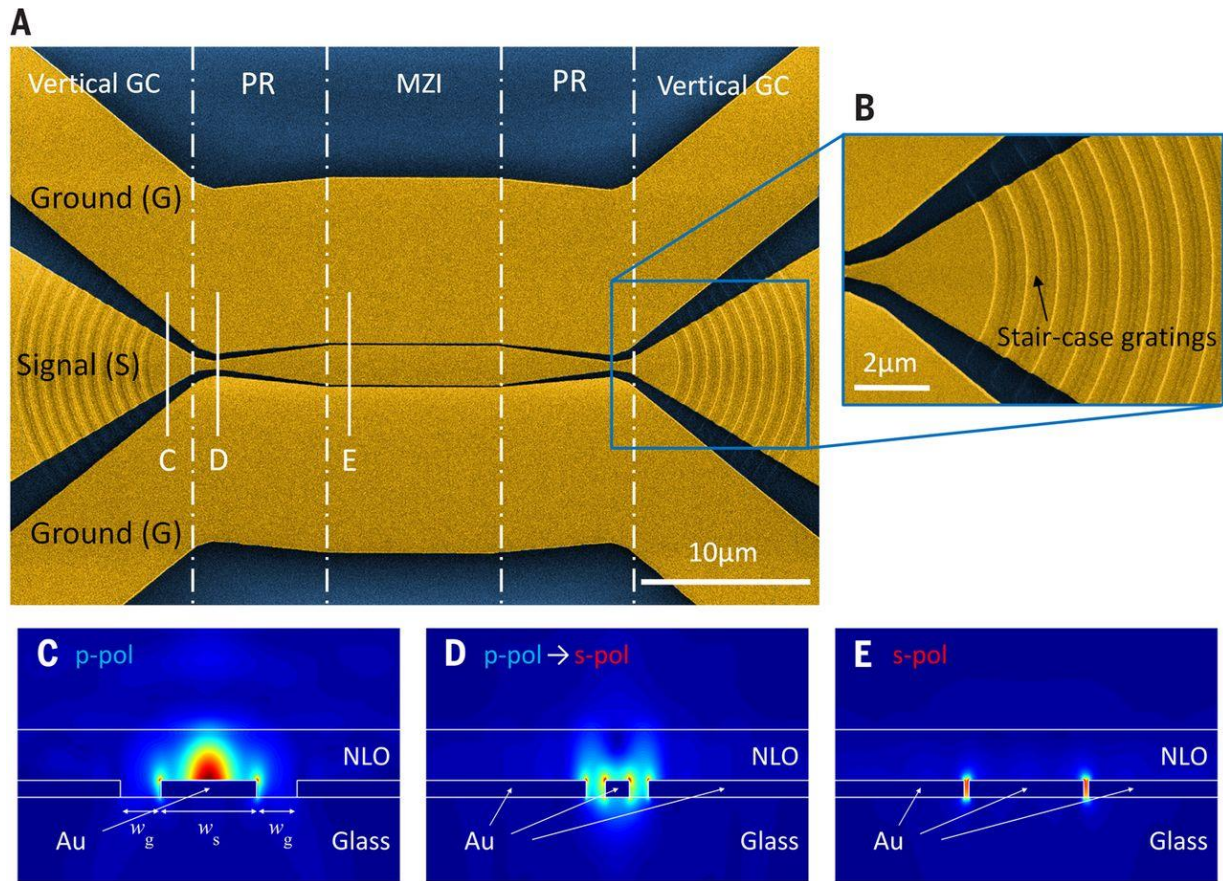


Fig. 2 Vertical grating coupler and polarization rotator of the all-metallic device.

(A) False-color scanning electron micrograph of the device fabricated in a single 200-nm-thick layer of gold (colored in yellow) deposited on thermally grown glass layer (dark blue). (B) Magnified image of a vertical metallic grating coupler with staircase gratings. The polarization rotation in the all-metallic device is illustrated by means of the plots of the electric field distributions. (C) A p-polarized surface plasmon polariton (SPP) on the top surface of the device after coupling through the vertical metallic grating coupler. (D) Conversion from p-polarized into s-polarized SPP mode in the polarization rotator section. (E) s-polarized SPP mode coupled into the metallic slot waveguides behind the polarization rotator section. The positions of the cross sections are shown in (A).

In an arrangement where space matters and the size of devices is far below a fiber diameter, a multicore fiber offers a solution for coupling light in and out. However, efficient coupling with a multicore fiber requires a vertical coupling scheme rather than the conventional tilted coupling schemes for taking advantage of the shortest possible pitch (14, 19, 32). Yet, coupling from a vertically aligned fiber mode with a 6-μm diameter to a plasmonic waveguide mode of a 100-nm width with a high efficiency is challenging. Conventional one-step-etch gratings would equally map the vertical-incident light into the forward and backward propagating modes (fig. S1). To enhance the coupling efficiency, we favor staircase gratings and break the horizontal symmetry (Fig. 2B). The staircase grating is composed of two diffraction points, creating waves that interfere constructively only in one direction but destructively in the other direction (33, 34).

We should note that only the p-polarized light can be coupled to the surface plasmon mode with a metallic grating coupler. For an efficient operation of the plasmonic modulator, however, it is necessary to squeeze the plasmonic mode as a gap plasmon into a metal-insulator-metal (MIM) waveguide (14, 18–21). Therefore, the polarization has to be rotated from p to s polarization. After light is coupled to the device via the grating coupler, the surface charges distribute mainly on the top surface of the central part of the waveguide, leading to p-polarization (Fig. 2C). The ratio between the two polarizations of the propagating light can be controlled by changing the widths of the signal pad  $w_s$  and the gap  $w_g$  of the waveguide (34). Therefore, when  $w_s$  and  $w_g$  decrease, the surface charges move along the sides and the s-polarization becomes dominant (Fig. 2D). Finally, the propagating mode is converted into two MIM waveguide modes with s-polarization by increasing  $w_s$  (Fig. 2E). In combination with a focusing



structure for the grating coupler, both the grating coupler and the polarization rotator can be arranged within a length of 15  $\mu\text{m}$ .

The devices were fabricated in a single layer of gold with a thickness of 200 nm and patterned by electron-beam lithography followed by dry etching of the metal. By replacing gold with copper, the device can be fabricated in a complementary metal-oxide semiconductor-compatible process. The devices were spin-coated with a nonlinear optical material (35), and poling processes were realized by applying a voltage between the ground electrodes. A detailed discussion on fabrication is provided in the supplementary materials (34).

Figure 3A shows the optical power transmission spectrum for different bias voltages, and Fig. 3B gives the optical transfer function versus the applied voltage. An extinction ratio of more than 15 dB has been found when switching from  $-6$  to  $+6$  V. The optical power transmission spectrum varies with the wavelength, and the spectrum shows a peak power around 1.55  $\mu\text{m}$  (Fig. 3A). This frequency dependence is due to the metallic gratings, which are optimized for that peak wavelength. Moreover, the spectrum features a wavelength dependence because of a built-in asymmetry in the two arms of the waveguides. Comparing the experimental transfer function in Fig. 3B with simulations, we extract the  $r_{33}$  electro-optic coefficient of the material and find that it is on the order of  $100 \text{ pm/V} \pm 15 \text{ pm/V}$ . Such a high extinction ratio with this voltage within only a few  $\mu\text{m}$  can be achievable because the device is arranged under an open-circuit MZI configuration in combination with a very strong light-matter interaction and a slow-down effect of plasmonic mode in the slots (21).

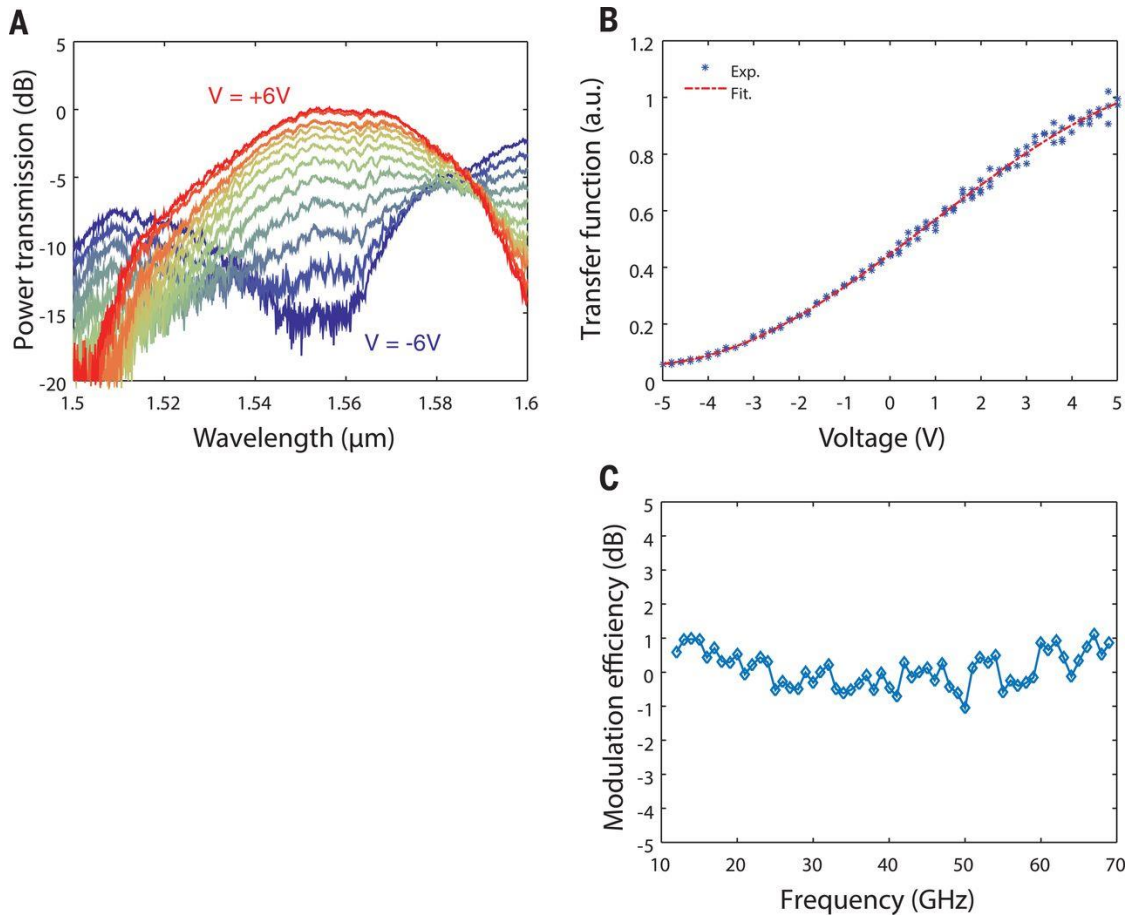


Fig. 3 Characterization of the all-metallic modulator.

(A) Optical power transmission spectrum for different bias voltages. (B) Optical power transfer function of the device over the applied voltage. (C) Normalized frequency response of the device.

The frequency response of the device (Fig. 3C) exhibits no speed limitation up to 70 GHz, which is the highest radio frequency (RF) signal currently available in our laboratory. The modulation bandwidth of a modulator can be estimated by the  $RC$  constant (the product of the circuit resistance and capacitance). Due to a very small capacitance (14 fF) (see the supplementary materials) and small resistances of the

device, the device should not be constrained for operation beyond 200 GHz. This indicates that the modulator is capable of dealing with fast electrical signals and thus should be able to provide the highest data transmission.

High-speed data experiments of the device have been performed using a continuous-wave (CW) optical signal at a wavelength of 1558 nm fed into the device (Fig. 4A). An arbitrary waveform generator was used to generate the 72 Gbit/s two-level pulse-amplitude modulation (PAM2) and 116 Gbit/s PAM4 modulation formats, respectively. This high-speed electrical signal was guided through electrical prober needles to the external electrical contact pads of the plasmonic modulator. The electrical signal was then encoded onto the surface plasmonic polariton, which was fed back to the multicore fiber. The transmitted signal was amplified and sampled by a coherent receiver before the digitized data were processed offline. The wide and open eye diagram with clearly distinct constellations of a PAM2 signal at 72 Gbit/s can be seen in Fig. 4B. A low BER of less than  $5.56 \times 10^{-6}$  was measured at this signal rate. The device was also tested for its performance with a higher-order modulation format. A PAM4 signal with a symbol rate of 58 GBd and a data rate of 116 Gbit/s was transmitted and detected with a BER of  $1.68 \times 10^{-3}$ . Both BERs are below the hard decision forward error correction (HD-FEC) limit of  $3.8 \times 10^{-3}$ , with a 7% overhead. Another important figure is the energy consumption of the modulator. Assuming that the energy consumption for a transition from one signal to the next costs  $CV^2/2$  (36), the estimated energy consumption is 110 fJ/bit with a driving voltage of  $\pm 2.8$  V at 72 Gbit/s for the PAM2 signal. If the advanced PAM4 signal is applied, the energy consumption drops to 30 fJ/bit at 116 Gbit/s (37). The fiber-to-fiber losses were found to be  $\sim 30$  dB rather than 17 dB as predicted by simulations (34). These excess losses are related to the applied fabrication technology and can be mitigated. Likewise, there is room for further reducing the losses, as discussed in the supplementary materials.

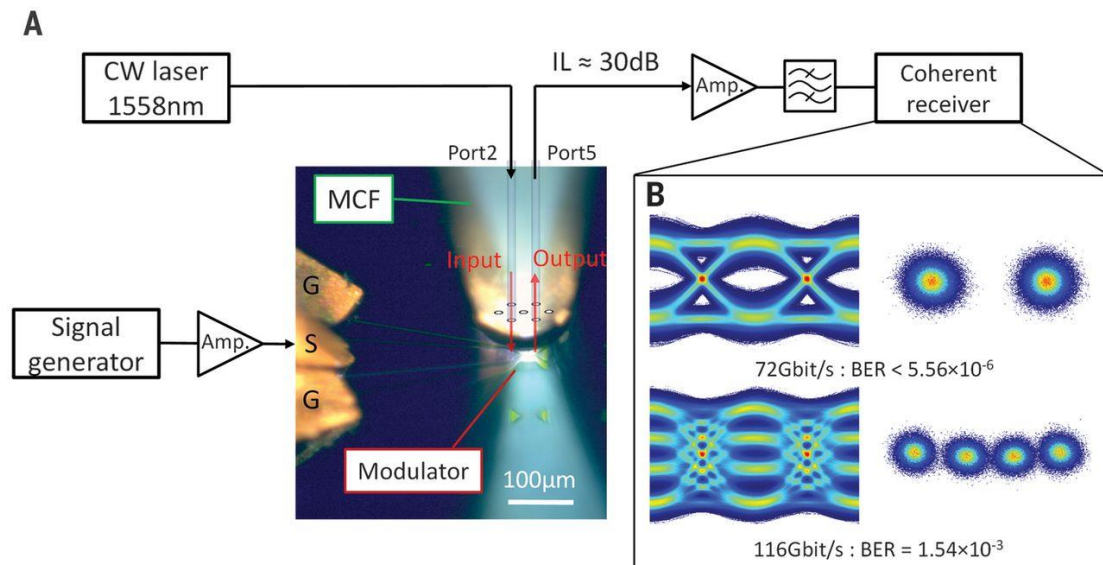


Fig. 4 High-speed data transmission experiment.

(A) Schematic of the data transmission experiment. (B) The eye diagrams and constellation diagrams of the 72 GBd PAM2 and 58 GBd PAM4 signals corresponding to a 72 Gbit/s and 116 Gbit/s data stream.

The work presented here shows that all-metallic devices can replace advanced optical configurations. Our all-metallic approach allows for a simple fabrication process with just one single metal layer and relaxed manufacturing requirements that addresses both operation speed and device footprint. The vertical multicore coupling solution enables a practical and dense way to directly interface plasmonics with electronics and might be an interesting packaging solution far beyond communications and sensing.

### Acknowledgments

This work was partially carried out at the Binnig and Rohrer Nanotechnology Center. We acknowledge support from European Union grant 688166 PLASMOFab and European Research Council grant 670478 PLASILOR. We thank A. Messner for support on temperature stability tests. Additional data can be found in the supplementary materials.